© MAY 2026 | IRE Journals | Volume 9 Issue 11 | ISSN: 2456-8880
DOI: https://doi.org/10.64388/IREV9I11-1718476

Effects Of Hybridization of Selected Agrowaste Fillers on the Thermal Properties of Epoxy-Based Composites

NORBERT N. NWORIE[1], OLISAEMEKA C. NWUFO[2], INNOCENT O. ARUKALAM[3], REMY UCHE[4]

[1]*Department of Mechanical Engineering, Federal Polytechnic Nekede, Owerri, Nigeria*
[2,4]*Department of Mechanical Engineering, Federal University of Technology, Owerri, Nigeria*
[3]*Department of Polymer Engineering, Federal University of Technology, Owerri, Nigeria.*

Abstract- ***The effects of hybridization of palm kernel fibre (PKF) and snail shell filler (SSF) on the thermal properties of epoxy-based composites were studied. The physico-chemical properties of PKF and SSF were evaluated using Fourier transform infrared (FTIR) spectroscopy. Differential scanning calorimetry (DSC) technique was employed to determine the melting and oxidation temperatures of the fabricated composites. The thermogravimetric analyzer (TGA) was used to assess the stability of the fabricated composites. From the stated assays, the FTIR results reveal that PKF contains cellulose, hemicellulose, and lignin, and the SSF has presence of calcium carbonate. DSC results showed that the use of hybrid fillers did not significantly influence the glass transition and melting temperatures of the composites. Further, the TGA results showed that the composite samples with hybrid natural fillers are slightly more thermally stable than the composites with single natural filler.***

Keywords: Composite, DSC, Hybridization, Palm Kernel Shell Fibre, Snail Shell Fibre.

I. INTRODUCTION

Due to scientific and technological advances, many of our modern technologies require materials with unusual combinations of properties that cannot be met by the conventional single metal alloys, ceramics, and polymeric materials (Kowser et al., 2023; Singh et al., 2024). To achieve this, more than one material, each consisting at least one required characteristic are brought together via already established composite processing technique(s). Thus, a composite is considered to be any multiphase material that exhibits a significant proportion of the properties of both constituent phases such that a better combination of properties is realized (Kumar and Kumar, 2023; Jumaidin et al., 2021). According to this principle of combined action, better property combinations are fashioned by the judicious combination of two or more distinct materials.

In addition, the constituent phases must be chemically dissimilar and separated by a distinct interface. The properties of composites are a function of the properties of the constituent phases - their relative amounts, and the geometry of the dispersed phase (Mohammed et al., 2023). In designing polymer-based composite materials, scientists and engineers have ingeniously combined various polymers with organic and/or inoroganic fillers to produce a new generation of improved materials.

Most polymer-based composites have been created to improve combinations of mechanical characteristics such as stiffness, toughness, ambient and high-temperature strengths (Balaji et al., 2022). This unique flexibility in design tailoring plus other attributes like ease of manufacturing, especially molding to any shape with polymer composites, repairability, corrosion resistance, durability, adaptability, cost effectiveness, etc. have attracted the attention of many users in several engineering and other disciplines (Seydibeyoğlu et al., 2023) to the use of composites.

Interestingly, synthetic polymers and fibres have found enormous applications in the fabrication of polymer-based composites, due to their inherent mechanical strength and low water absorption, among others (Fox et al., 2016). Additionally, purely sythetic fibres used for structural composite applications pose environmental threat after their service life, due to their inability to degrade. To reduce enviromental pollution caused by these non-

degradable waste synthetic fibres and ensure environmental sustainability, there is need to develop high performance biodegrable polymer-based composites for structural applications.

Thus, the use of natural fibres as reinforcements in polymer-based composites offers potential benefits in terms of sustainability and reduced environmental impact compared to synthetic fibres (Kozynets et al., 2023; Chen et al., 2023; Kumar et al., 2014). On the basis of cost-effectiveness, natural fibres generally have lower production costs compared to synthetic fibres. Natural fibres are renewable, biodegradable, and have lower carbon footprints. Based on the performance enhancement, understanding the thermal properties of natural fillers and their compatibility with polymer matrices such as epoxy is essential for designing composite materials with enhanced thermal performance.

To further enhance the performance applications of natural fibre-based epoxy composites, hybridization of natural fibres in epoxy composites have shown that it can exhibit synergistic effects that can lead to further performance improvements (Demir et al., 2023; Olaitan et al., 2017;). For example, hybrid fibres-based composites can exhibit superior mechanical properties, enhanced thermal stability, and tailored characteristics compared to single-fibre composites.

Considering the given literatures, the present study aims to study the effects of hybridization of palm kernel shell fibres and snail shell fibres on the thermal properties of epoxy-based composites for structural applications. The thermal properties analysis using differential scanning calorimetry (DSC) technique was employed to determine the melting and oxidation temperatures of the fabricated composites. Also, the thermogravimetric analysis (TGA) was conducted to appraise the thermal stability of the composites.

II. MATERIALS AND METHOD

2.1 Materials

Epoxy resin and hardner were used as the matrix. Palm kernel shell fibre and snail shell fibre were used as natural filler materials, whilere aluminium oxide was used as synthetic filler. Aminopropyl trimethoxy silane were used as surface modification agent to enhance the hydrophobicity of the fibres and ensure fibre-epoxy matrix adhesion.

2.2 Method

2.2.1 Collection and pulverization of palm kernel and snail shells

Palm kernel shells shown in Plate 1(a) were locally procured from oil palm milling sites. The shells were pulverized using locally fabricated crushing machine and sieved. The obtained particles were further pulverized using a ball milling machine and then sieved to obtain fine powdered palm kernel shell particles. The resulting palm kernel fibres were mixed with 2 wt.% of aminopropyl trimethoxy silane, oven-dried for 2 hours, retrieved and then stored in a dessicator before use.

Similarly, the snail shells shown in Plate 1(b) were procured from dumpsites close to seafoods section at Worldbank market Owerri. They were washed, dried and pulverized into fine powder using locally fabricated crushing machine. Subsequently, the pulverized snail shells were oven-dried at 70 °C for 2 hs. Thereafter, the sample was retrieved, allowed to cool for 30 min at room temperature and then further pulverized using a ball milling machine and sieved to obtain free-flowing snail shell powder. The resulting pam kernel fibres were mixed with 2 wt.% of aminopropyl trimethoxy silane, oven-dried for 2 hours, retrieved and then stored in a dessicator prior to use.

Plate 1: (a) Palm kernel shells, and (b) snail shells

2.2.2 Composite fabrication

The composite was fabricated using epoxy resin and hardner, hybrid formulations consisting of two natural fillers (palm kernel shell fibre and snail shell filler) and aluminium oxide as synthetic filler. Based

on the formulation given in Table 1, each of the composite formulations was mixed with 1 wt.% aminopropyl trimethoxy silane using a kitchen blender. Thereafter, each of the resulting composite formulation was fabricated by casting method. After product formation, the composite was retrieved, and allowed to cure at ambient temperature for 72 hs. The composites were then kept in a dessicator prior to appropriate characterization.

Table 1: Epoxy-based composites using varying amounts of natural fillers

Sample ID	Epoxy matrix (wt. %)	Synthetic filler Al_20_3 (wt. %)	Natural filler (wt. %)		Silane coupling agent (%)
			PKF	SSF	
1	100	0	0	0	0
2	80	9	10	0	1
3	60	9	30	0	1
4	40	9	50	0	1
5	80	9	0	10	1
6	60	9	0	30	1
7	40	9	0	50	1
8	80	9	5	5	1
9	60	9	15	15	1
10	40	9	25	25	1

2.2.3 Characterizations

(a) Thermal properties tests

(i) Differential Scanning Calorimetry (DSC)

An empty reference pan was placed on the reference side of the DSC instrument, while small amount of each of the samples (natural fillers and epoxy-based composites) was placed in the sample pan.

Thereafter, the chamber lid was closed, and the DSC control software was opened. The essential details such as the sample mass, sample name, test parameters such as start temperature, heating/cooling rates, maximum temperature and other relevant information were entered. The file name and data storage location were entered. Following the programmed inputs, the test was initiated by clicking the start button. Thus, the DSC measures the difference in heat flow required to maintain equal temperatures between the sample and reference. This data was recorded as thermograms. Hence, the melting temperature and absorbed heat energy could be determined.

(ii) Thermogravimetric Analysis (TGA)

The mass of each of the samples (natural fillers and epoxy-based composites) was measured and placed on the sample pan of the thermogravimetric analyzer (TGA). The TGA instrument was programmed to heat the sample from the room temperature to 400, 500, 600 and 700 oC, depending on the sample involved. The heating rate was set at 20 °C/minute.

The test was initiated by clicking the start button on the TGA instrument. The TGA generated thermogravimetric curves which plotted the percentage of weight loss against the temperature. Thus, the oxidation and degradation temperatures of the samples were obtained.

(b) Fourier Transform Infrared (FT-IR) Spectroscopy Analysis

The FTIR spectra of the pulverized palm kernel shell and snail shell fillers were acquired in the range of 450–4000 cm−1 wavenumber by use of PerkinElmer Spectrum IR spectrophotometer, version 10.7.2. The procedure involved mixing 4 mg each of the pulverized palm kernel shell and snail shell fillers with 100 mg of pure anhydrous KBr.

The mixture was ground to fine powdered form using a mortar and a pestle. Each of the ground mixture was then placed onto a circular disk and pressed into a transparent flake. Subsequently, it was placed into the detection chamber of IR spectrophotometer with a sample holder, and the IR spectra were recorded with the Omnic software at a resolution of 4 cm−1, with 64 scans and a gain of 1.

III. RESULTS AND DISCUSSION

3.1 Processing of palm kernel fibres and snail shells fillers

The pulverized palm kernel and snail shells shown in Plate 2 were sieved with 150 μm size mesh. Micro observation of the fillers revealed fine particulate fillers. However, a closer observation of the pulverized palm kernel shell, snail shell revealed a heterogeneous mix of irregular fillers which reflects the fibrous nature of palm kernel shell, while the

snail shell fillers maintain their particulate nature that are generally non-spherical. Generally, the two fillers exhibited a rough surface texture due to the breaking and fragmentation of the shell structure.

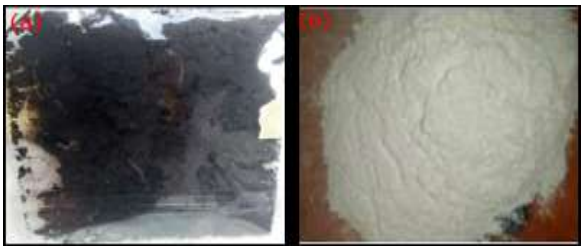

Plate 2: (a) Pulverized palm kernel shells, and (b) pulverized snail shells

3.2 Thermal properties of palm kernel fibres and snail shells fillers

The thermal property analysis was conducted using differential scanning calorimetry (DSC) and thermogravimetric analysis (TGA) to establish the melting and decomposition temperatures of the palm kernel and snail shells in order to gain insight into service operation of the products that would contain them.

(a) Differential scanning calorimetry (DSC)

DSC measures heat flow into or out of a sample as it is heated or cooled. When a material oxidizes, it releases heat, causing an exothermic peak on the DSC curve. The oxidation onset temperature (OOT) is the specific temperature at which this exothermic peak begins, indicating the start of the oxidation process. It indicates a material's resistance to oxidation, with higher OOT values signifying greater stability. The oxidation temperature (OT), is the temperature at which a material begins to oxidize, releasing heat (exothermic reaction) to the environment.

Thus, the DSC scan of palm kernel shell powder given in Figure 1 shows a phase change at 122.83 oC with enthalpy of 3.976 J/g. As the scan temperature increased, an oxidation onset temperature (OOT) was oberved at 187.38 oC. Finally, an oxidation temperature (OT) at 252.75 oC.

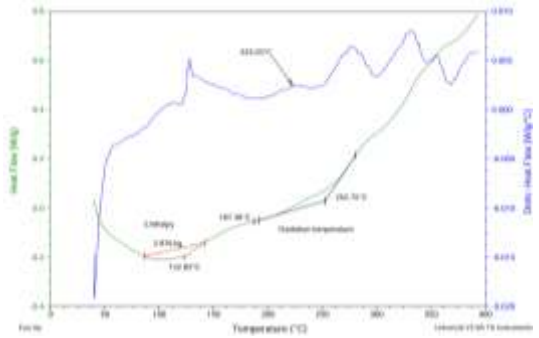

Figure 1: DSC thermogram for the pulverized palm kernel shell filler

Further, the Figure 2 depicts the DSC thermogram of snail shell powder. From the Figure 2, it could be observed that there was a little phase change that occurred between 65 and 125 oC. Thereafter, the oxidation onset temperature and oxidation temperature were observed at 207.92 and 280.56 oC, respectively.

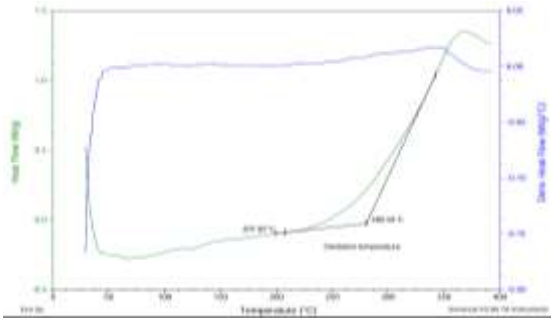

Figure 2: DSC thermogram for the pulverized snail shell filler

(b) Thermogravimetric Analysis (TGA)

Figure 3 depicts the TGA thermogram of the palm kernel shell powder. It shows that palm kernel shell underwent thermal degradation in three distinct phases. The first step decomposition phase occurred between 26.19 and 161.53 oC, where dehydration took place. The second step decomposition occurred between 161.53 and 796.10 oC, where degradation of hemicellulose and cellulose occurred. In this step, there was a significant mass loss of 1.79 mg corresponding to 78.02 %. Finally, the degradation of lignin occurred between 796.10 and 994.84 oC. This phase involved the breaking of chemical bonds and the formation of ash residue.

© MAY 2026 | IRE Journals | Volume 9 Issue 11 | ISSN: 2456-8880
DOI: https://doi.org/10.64388/IREV9I11-1718476

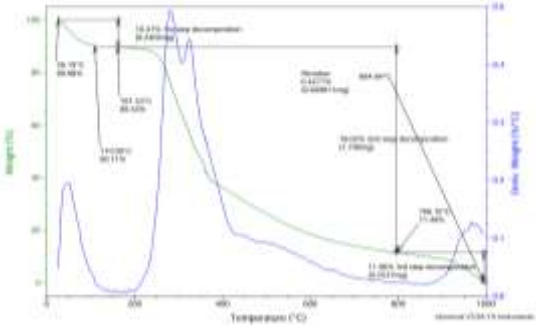

Figure 3: TGA thermogram for the pulverized palm kernel shell filler.

Furthermore, the TGA thermogram for the snail shell powder is shown in Figure 4. The first step decomposition phase occurred at temperatures between 45.42 and 200.88 oC. In this phase, a small amount of mass loss occurred, which is attributed to the removal of moisture and residual organic matter. The second step decomposition phase occurred at temperatures between 200.88 and 528.75 oC. This corresponds to the decomposition of organic components such as proteins and carbohydrates that bind the calcium carbonate. The third step decomposition occurred at temperatures between 528.75 and 798.12 oC. A significant mass loss occurred within this temperature range. This is the calcination stage that represents the thermal decomposition of calcium carbonate (CaCO3) into calcium oxide (CaO) and carbon dioxide (CO2).

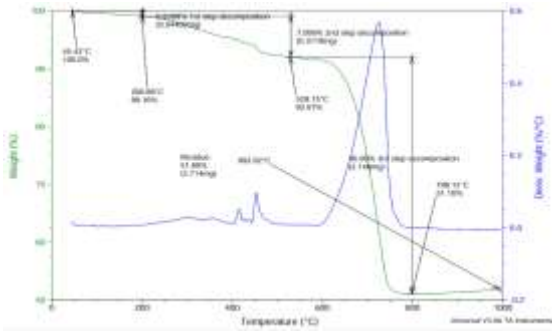

Figure 4: TGA thermogram for the pulverized snail shell filler

In summary, from the results given above, it be could be observed that palm kernel shell powder can be thermally stable up to the temperature of 796.10 oC, whereas the snail shell powder is thermally stable at 798.12 oC.

3.3 Fourier transform infrared (FT-IR) results for palm kernel and snail shells

The pulverized palm kernel shells, snail shells and wood fibres were characterized using FT-IR technique. Subsequently, the results of the characterization are given in Figure 5 and Figure 6 for the pulverized palm kernel shells and snail shells, respectively.

Figure 5 shows large FT-IR absorption peak at 3352.04 cm-1 which is associated to O–H stretching. This absorption is attributed to the hydroxyl (O–H) groups present in the lignocellulosic components (cellulose, hemicellulose, and lignin) of the palm kernel shell. The spectrum at 1629.87 cm-1 corresponds to C=C stretching which indicates the presence of aromatic rings and conjugated double bonds within the palm kernel shell structure, particularly from lignin.

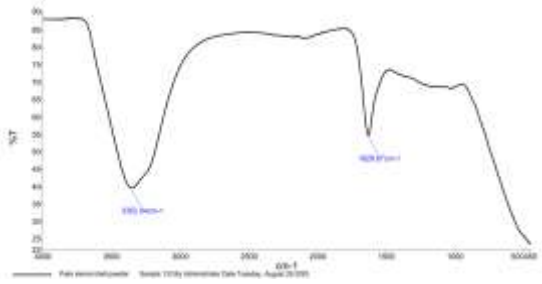

Figure 5: FT-IR spectra of pulverized palm kernel shell fibre

Further, it has been established that the FT-IR spectra of snail shell powder show characteristic absorption bands for the carbonate ions (CO_3^{2-}) typically in the range of 700–1800 cm^{-1}, indicating the presence of calcium carbonate, which is the primary component of snail shells (Anjaneyulu, Pattanayak and Vijayalakshmi, 2015). However, Figure 6 presents FT-IR spectra for the pulverized snail shell filler, with characteristic absorption bands at 699.89, 712.51, 857.27, 1082.98 and 1468.28 cm^{-1} corresponding to the carbonate ions. A good observation of the spectrum clearly reveals the absence of moisture in the snail shell powder.

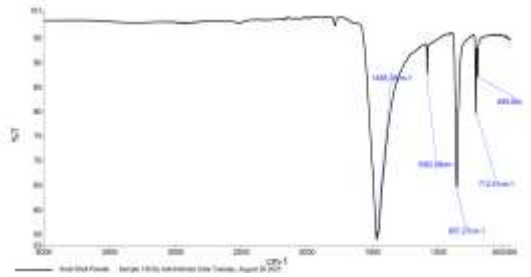

Figure 6: FT-IR spectra of pulverized snail shell filler

3.4 Thermal properties of fabricated composite samples

The determination of glass transition temperature (Tg) of a material is crucial because it defines the critical temperature range where a material's properties change dramatically from a hard, brittle glassy state to a soft, flexible rubbery state (Lungulescu et al. 2022; Gijsman and Fiorio, 2023).

This information allows for precise control over material selection, product design, processing parameters, and quality assurance. Therefore, understanding a material's Tg is essential for predicting and optimizing its performance, durability, and manufacturability for its intended applications. Therefore, a high glass transition temperature (Tg) implies that the material will remain rigid and brittle, at higher operating temperatures before softening, while a low Tg implies that the material will be soft, flexible, and rubbery at lower temperatures.

On the other hand, melting temperature determination is essential for confirming the identity of a solid substance and assessing its purity (Darsaklis 2025). Thus, a pure substance has a sharp, constant melting point, while impurities lower and broaden this range. This analysis serves as a vital quality control tool, and provides essential information for characterizing materials and establishing processing conditions. Therefore, a high melting temperature implies strong intermolecular forces which requires more energy to break, while a low melting temperature indicates weaker forces and suggests the presence of impurities.

Further, determining oxidation temperature (OT) is vital for assessing material stability and predicting its lifetime, as it identifies the temperature at which a material begins to chemically degrade through oxidation (Xie et al. 2020). The oxidation onset temperature (OOT) provides a relative measure of a material's resistance to oxidative decomposition.

In view of the above established facts, the thermal events – glass transition, melting, and oxidation for the fabricated composite samples which were determined using differential scanning calorimetry technique are given in Figure 7.

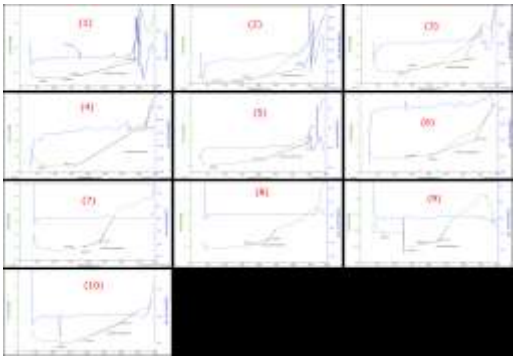

Figure 7: Results of differential scanning calorimetry on the plain epoxy and fabricated composite samples

From the DSC thermograms in the Figure 7, the values of glass transition temperatures, melting temperatures, oxidation onset temperatures and oxidation temperatures were extracted and presented in Table 2.

Table 2: DSC values of glass transition temperature (Tg), melting temperature (Tm), oxidation onset temperature (OOT), and oxidation temperature for selected composite samples.

Sample ID	1	2	3	4	5	6	7	8	9	10
Tg (°C)	69.76	73.44	56.13	62.07	67.44	65.52	55.17	49.85	68.65	63.50
Tm(°C)	124.54	121.91	118.44	120.75	118.75	134.83	154.20	112.50	126.76	121.91
OOT(°C)	177.96	169.35	133.98	162.47	212.63	207.83	188.60	188.33	195.96	176.72
OT (°C)	335.88	334.85	300.59	373.78	341.92	335.45	235.42	223.99	228.47	293.34

Hence, the plain epoxy sample 1 has a Tg of 69.76 oC. When compared to the Tg of the composite samples 2 – 10, it is only sample 2, which is the composite sample with 10 wt.% PKF as the only natural filler in it that has a higher Tg of 73.44 oC, and sample 9 that has almost equal Tg with the sample 1. Other composite samples have Tg lower than that of the plain epoxy sample 1. What this means is that sample 2 is most rigid of all the samples, and it is suitable for applications where higher operating temperature is required. It further implies that the sample 2 has greater stability and a reduced susceptibility to deformation. On the other hand, the composite samples with Tg quite lower than that of the plain epoxy sample 1, ought to be softer and more flexible than the sample 1. If otherwise, it should be attributed to agglomeration and poor dispersion of constituent materials.

The melting temperature (Tm) of sample 1 was obtained to be 124.54 oC. Comparing the Tm of sample 1 to the melting temperatures of the composite samples, samples 6, 7, and 9 which have higher Tm values, should have higher intermolecular forces, and therefore should be used where applications requiring high temperature is needed.

On the other hand, the thermogravimteric analyses (TGA) results of the fabricated composites are depicted in Figure 8.

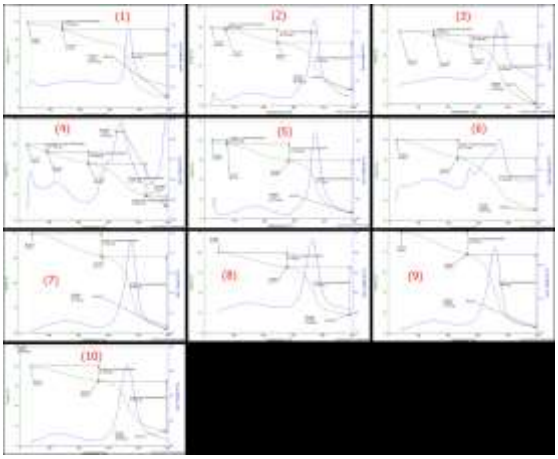

Figure 8: Results of thermogravimetric Analysis on the plain epoxy and fabricated composite samples

From the Figure 8, the first step decomposition (FSD) temperature, second step decomposition (SSD) temperature, third step decomposition (TSD) temperature and fourth step decomposition (4thSD) temperature for sample 1 and the fabricated composite samples were extracted and listed in Table 3.

Table 3: TGA values of first step decomposition (FSD) temperature, second step decomposition (SSD) temperature, third step decomposition (TSD) temperature and fourth step decomposition (4thSD) temperature for selected composite samples.

Sample ID	1	2	3	4	5	6	7	8	9	10
FSD	24.93 – 142.19	24.90– 72.19	37.15– 153.34	27.10– 93.79	24.40– 76.23	23.99– 233.10	41.66– 275.98	47.98– 279.00	41.66– 263.87	36.65 – 266.90
SSD	142.19 –305.25	72.19– 246.22	153.34– 275.29	93.79– 232.28	76.23– 282.03	233.10– 492.88	275.98– 494.39	279.00– 492.38	263.87– 494.90	266.90– 494.39
TSD	305.25– 494.40	246.22– 493.89	275.29– 492.23	232.28– 424.64	282.03– 493.39	–	–	–		
4^{th}SD				424.64– 494.24						

The obtained TGA values have a broad range, which indicates presence of impurities in the samples. The first step decomposition phase is the common stage where dehydration of moisture and residual organic matter occurred. The second step decomposition phase for the composite samples with only PKF natural filler is where degradation of hemicellulose and cellulose occurred. In this second step decomposition phase, the composite samples with only SSF natural filler shows degradation of proteins and carbohydrates that bind the calcium carbonate together. For the composite samples with hybrid

natural fillers, the second step decomposition denotes degradation of hemicellulose, cellulose, proteins and carbohydrates.

The third step decomposition phase for the composites only PKF natural filler and the composite samples with only SSF natural filler presents degradation of lignin and thermal decomposition of calcium carbonate, respectively. For the composite samples with hybrid natural fillers, the third step decomposition phase shows degradation of lignin and decomposition of calcium carbonate. However, interestingly, sample 4 exhibited fourth step decomposition phase, and this denotes degradation of lignin into volatile products and a residual solid char.

Further, the results of thermogravimteric analysis (TGA) can be used to evaluate the thermal stability of a material. TGA records change in mass from dehydration, through decomposition to oxidation of a material with time and temperature. It is also used to study reactions, kinetics, material's properties, and residual substances. If a material is thermally stable, there will be no observed mass change. However, negligible mass loss corresponds to little or no slope in the TGA curve, and implies that the material under investigation is thermally stable.

The TGA was also used to measure the mass losses of the plain epoxy sample 1 and the composite samples as function of temperature under predefined programme. The thermograms for the TGA determinations are given in Figure 8. As presented in the thermograms in Figure 8, sample 1 appears to be thermally stable at 400 oC, while sample 2 around 493.89 oC, sample 3 is at 492.23 oC, sample 4 at 493.18 oC, sample 5 at 493.39 oC, sample 6 at 492.88 oC, sample 7 at 494.39 oC, sample 8 at 492.38 oC, sample 9 at 494.90 oC, and sample 10 at 494.39 oC. This is because at these temperatures, there were no mass losses in the corresponding materials.

IV. CONCLUSION

The effects of hybridization of palm kernel and snail shell agrowaste fillers on the thermal properties of epoxy-based composites have been conducted. Based on DSC results, the use of hybrid fillers did not significantly influence the glass transition and melting temperatures of the composites. The TGA results have shown that the composite samples with hybrid natural fillers are slightly more thermally stable than the composites with single natural filler.

V. ACKNOWLEDGEMENT

The authors were grateful to Dr. Q. Ochieze for his assistance in the characterization of some samples. We are equally grateful to the laboratory Technologists at the Department of Mechanical Engineering, Federal University of Technology Owerri (FUTO) for their assistance during the composite preparation. Finally, the authors are grateful to the School of Engineering and Engineering Technology and School of Postgraduate Studies, FUTO.

REFERENCES

[1] Anjaneyulu U., Pattanayak D.K. and Vijayalakshmi U. Snail Shell Derived Natural Hydroxyapatite: Effects on NIH-3T3 Cells for Orthopedic Applications. Materials and Manufacturing Processes, 2015. DOI: 10.1080/10426914.2015.1070415.

[2] Balaji A., Kannan S., Purushothaman R., Mohanakannan S., Maideen A.H., Swaminathan J., Karthikeyan B., Premkumar P. Banana fiber and particle reinforced epoxy biocomposites: mechanical, water absorption, and thermal properties investigation, Biomass Conversion and Biorefinery, 2022, 14(6):1-11. https://doi.org/10.1007/s13399-022-02829-y.

[3] Chen T., Ma Q., Li Y., Li G. Preparation and Characterization of Wood Composites for Wood Restoration, Forests (2023), 14, 1743. https://doi.org/10.3390/f14091743.

[4] Darsaklis I. Identification of an Unknown Organic Compound by Determination of its Melting Point, International Journal of Scientific Research in Chemical Sciences, 2025, 12(1):28-32. DOI:10.26438/ijsrcs. v12i1.184

[5] Demir O, Yar A, Eskizeybek V, Avcı A. Combined effect of fiber hybridization and matrix modification on mechanical properties of polymer composites. Proceedings of the

Institution of Mechanical Engineers, Part L: Journal of Materials: Design and Applications. 2023;237(9):1935-1951. doi:10.1177/14644207231162547.

[6] Fox D., Kaufman N., Woodcock J.W., Davis C., Gilm J.W., Shields J.R., Davis R. Matko S., Zammarano M. Epoxy Composites Using Wood Pulp Components as Fillers, 2016. DOI: 10.5772/65261

[7] Gijsman P. and Fiorio R. Long term thermo-oxidative degradation and stabilization of polypropylene (PP) and the implications for its recyclability, Polymer Degradation and Stability, 2023, 208(110260). https://doi.org/10.1016/j.polymdegradstab.2023.110260.

[8] Jumaidin, R.; Diah, N.A.; Ilyas, R.A.; Alamjuri, R.H.; Yusof, F.A.M. Processing and Characterisation of Banana Leaf Fibre Reinforced Thermoplastic Cassava Starch Composites. Polymers, 2021, 13, 1420. https://doi.org/10.3390/ polym13091420.

[9] Kowser, M.A.; Hossain, S.M.K.; Amin, M.R.; Chowdhury, M.A.; Hossain, N.; Madkhali, O.; Rahman, M.R.; Chani, M.T.S.; Asiri, A.M.; Uddin, J.; Rahman, M.M. Development and Characterization of Bioplastic Synthesized from Ginger and Green Tea for Packaging Applications. J. Compos. Sci. 2023, 7, 107. https://doi.org/10.3390/jcs7030107.

[10] Kozynets S., Starokadomsky D., Reshetnyk M., Kokhtych L., and Bodul N. Eco-Biocompatible Epoxy Composites with Vegetable Fillers, Biomed J Sci & Tech Res, 2023, 50(4). BJSTR.MS.ID.007973.

[11] Kumar, N., Kumar, J. Investigation of machining characteristics and surface integrity for trim cut WEDM of hybrid metal matrix composite [Al 6061, SiC, and TiB2]. J. Eng. Appl. Sci. 2023, 70, 117. https://doi.org/10.1186/s44147-023-00289-3.

[12] Kumar R., Kumar K., Sahooc P., and Bhowmik S. Study of Mechanical Properties of Wood Dust Reinforced Epoxy Composite, Procedia Materials Science, 2014, 6:551 – 556.

[13] Lungulescu, E.-M., Setnescu, R., Ilie, S., and Taborelli, M. On the Use of Oxidation Induction Time as a Kinetic Parameter for Condition Monitoring and Lifetime Evaluation under Ionizing Radiation Environments. Polymers, 2022, 14(12), 2357. https://doi.org/10.3390/polym14122357.

[14] Mohammed M., Oleiwi J.K., Mohammed A.M., Jawad A.J.M., Osman A.F., Adam T., Betar B.O., Gopinath S.C.B., Dahham O.S., Jaafar M. Comprehensive insights on mechanical attributes of natural-synthetic fibres in polymer composites, Journal of Materials Research and Technology, 2023, 25, 4960-4988. https://doi.org/10.1016/j.jmrt.2023.06.148.

[15] Olaitan A.J., Ufuoma O.D., King G.D. and Raphael O. Production of a safety helmet, palm kernel fibre and shell particulates, International Journal of Engineering Science Invention, 2017, 6(2):44-55.

[16] Seydibeyoğlu M.Ö., Dogru A., Wang J., Rencheck M., Han Y., Wang L., Seydibeyoğlu E.A., Zhao X., Ong K., Shatkin J.A., Shams Es-Haghi S., Bhandari S., Ozcan S., Gardner D.J. Review on Hybrid Reinforced Polymer Matrix Composites with Nanocellulose, Nanomaterials, and Other Fibers. Polymers (Basel), 2023, 15(4):984. doi: 10.3390/polym15040984.

[17] Singh P., Sheikh J., Behera B.K. Metal-faced sandwich composite panels: A review. Thin-Walled Structures, 2024, 195, 111376.

[18] Xie R., Weisen A.R., Lee Y., Aplan M.A., Fenton A.M., Masucci A.E., Kempe F., Sommer M., Pester C.W., Colby R.H., Gomez E.D. Glass transition temperature from the chemical structure of conjugated polymers. Nat Commun. 2020, 14;11(1):893. doi: 10.1038/s41467-020-14656-8.